Kinetics of Tyrosyl Radical Reduction by Selenocysteine

Daniel Steinmann,[‡] Thomas Nauser,[‡] Joris Beld,[§] Martin Tanner,[‡] Detlef Günther,[‡] Patricia L. Bounds,[‡] and Willem H. Koppenol*[,‡]

Laboratories of Inorganic and Organic Chemistry, Department of Chemistry and Applied Biosciences, ETH Zurich, 8093 Zurich, Switzerland

Received June 1, 2008; Revised Manuscript Received July 11, 2008

ABSTRACT: The rate constant for the reduction of the tyrosyl radical with selenocysteine has been measured to investigate whether selenocysteine is capable of repair of protein radicals. Tyrosyl radicals, both free in solution and in insulin, were generated by means of pulse radiolysis and laser flash photolysis in aqueous solution. The rate constant for the reaction of free *N*-acetyl-tyrosyl-amine radicals with selenocysteine is $(8 \pm 2) \times 10^8$ M^{-1} s^{-1}, and that for tyrosyl radicals in insulin is $(1.6 \pm 0.4) \times 10^8$ M^{-1} s^{-1}. The rate constant for the reaction of selenoglutathione with the *N*-acetyl-tyrosyl-amine radical is $(5 \pm 2) \times 10^8$ M^{-1} s^{-1}. In contrast, cysteine and glutathione react more slowly than their selenium analogues with the tyrosyl radical: the reactions of *N*-acetyl-tyrosyl-amine radicals with cysteine and glutathione are 3 and 5 orders of magnitude slower, respectively, than those with selenocysteine and selenoglutathione, while those of tyrosyl radicals in insulin are 3 and 2 orders of magnitude slower, respectively.

In mitochondria, ca. 1% of the dioxygen processed during oxidative phosphorylation is reduced to the superoxide radical anion instead of water, and subsequent radical reactions can damage cellular biomolecules. Proteins are frontline targets of these radical reactions: the one-electron oxidation of an amino acid may result in a short chain of reactions, in which the initial amino acid radical is repaired by a series of other amino acid residues to form more thermodynamically stable species (*2*), to ultimately generate the tyrosyl radical, which is the least reactive of all amino acid radicals (*3*−*5*). The tyrosyl radical tends to undergo repair, to dimerize, or to form a covalent bond with another amino acid (*6, 7*). Unlike other amino acid radicals, the tyrosyl radical reacts with oxygen relatively slowly ($k < 1 \times 10^3$ M^{-1} s^{-1}) (*8*); thus, its lifetime can be considerable, as in ribonucleotide reductase, where a tyrosyl radical plays an essential role in the enzyme reaction mechanism (*9*). Covalent bonds between tyrosine and cysteine (*10*) and between tyrosine and histidine (*11*−*13*) have been observed in fully functional proteins, e.g., galactose oxidase, catalase, and cytochrome *c* oxidase. Tyrosyl−cysteine or tyrosyl−histidine bonds arise after formation of a cysteinyl or histidinyl radical, followed by reaction with a nearby tyrosine side chain and subsequent oxidation of the radical tyrosine adduct by a neighboring copper and/or iron redox center. In other proteins, tyrosyl radicals formed in response to oxidative stress are thought to impair protein structure and/or function and could propagate damage to other cellular components.

Our findings regarding the redox properties of selenocysteine (Sec),[1] the selenium analogue of cysteine (*14*), led us to suspect that Sec can act as an antioxidant without propagating damage. According to our working hypothesis, Sec$^\bullet$ formed during repair of a protein radical by Sec would react with another Sec or Cys to form a diselenuidyl $(Se\therefore Se)^{\bullet-}$, or a mixed selenium−sulfur radical $(S\therefore Se)^{\bullet-}$. Such a radical species would be a target for oxidation by dioxygen, and the superoxide so formed would be eliminated by superoxide dismutase, a cascade of reactions known as the superoxide-sink pathway (*15*). The reduction of dioxygen by the diselenuidyl radical is so favorable that this cascade is essentially irreversible (*16*).

The electronegativity of selenium is somewhat smaller than that of sulfur and its ionic radius somewhat larger, and the accessible oxidation states are comparable. On the basis of these considerations, selenium could replace sulfur in biomolecules. Indeed, enzymes that contain Cys at the active site in certain organisms contain Sec in corresponding enzymes in other organisms. However, selenium is more easily oxidized (*14*), and Sec is, in contrast to Cys, fully deprotonated at physiological pH. Although substitution of Sec for Cys in a protein is likely to alter its functionality, the evolutionary driving forces behind the relative functionalities of Sec and Cys in enzymes are not fully understood (*17*).

By means of proteome analysis, 25 human selenoproteins have been identified (*18*). Although the functions of the

[†] We thank the ETH for financial support.

* To whom correspondence should be addressed. E-mail: koppenol@inorg.chem.ethz.ch. Telephone: +41 44 632 28 75. Fax: +41 44 632 10 90.

[‡] Laboratory of Inorganic Chemistry.

[§] Laboratory of Organic Chemistry.

[1] Abbreviations, systematic nomenclature (trivial names): $N_3^\bullet$, trinitrogen$^\bullet$ (azide radical); Sec, selenocysteine; Sec_{ox}, selenocystine; Sec$^\bullet$, selenocysteinyl radical; $(Se\therefore Se)^{\bullet-}$, diselanuidyl$^{\bullet-}$ (diselane radical anion, diselenide radical anion); GSH, glutathione; GSeH, selenoglutathione. The *G* value represents the number of specified chemical events (production of radicals) produced in an irradiated substance per 100 eV of energy absorbed from ionizing radiation. A *G* of 1 corresponds to 0.1036 μmol dm^{-3} J^{-1}.

10.1021/bi801029f CCC: $40.75
Published on Web 08/15/2008

Scheme 1

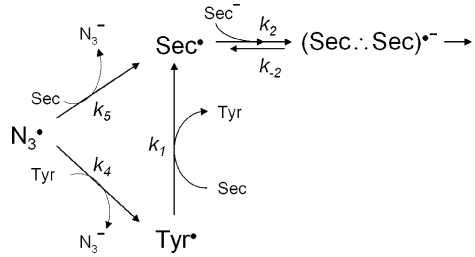

majority of selenoproteins discovered to date are unknown (*19*), most are redox enzymes that exert their catalytic activity via Sec. Examples include glutathione peroxidases, which reduce peroxides and catalyze disulfide−thiol interconversion, and thioredoxin reductases, which reduce numerous substrates, most importantly, thioredoxin [a small protein that in turn acts as a general protein disulfide reductant (*19*)]. Further characterized proteins are the selenoprotein R, which catalyzes the reduction of oxidized methionine, the selenophosphate synthases involved in Sec biosynthesis, and the iodothyronine deiodinases, a family of selenoenzymes that control thyroid hormone metabolism. A variety of functions have been postulated for selenoprotein P, including chelation of heavy metals, transport of selenium to organs, and, more recently, scavenging of oxidants.

We show here that tyrosyl radicals (Tyr$^•$), both in *N*-Ac-Tyr-NH_2 and in the protein insulin, react with Sec (reaction 1) and selenoglutathione (GSeH) in aqueous solution at pH 7.4 with second-order rate constants on the order of 10^8-10^9 M^{-1} s^{-1}, 2−5 orders of magnitudes faster than with the corresponding sulfur compounds.

$$Tyr^• + Sec^- \rightarrow Tyr^- + Sec^• \quad (1)$$

Our findings indicate that Sec may have the potential to effectively repair Tyr$^•$ radicals (Scheme 1).

EXPERIMENTAL PROCEDURES

Chemicals. Millpore MilliQ water (18.2 MΩ) was used in all experiments. Chemicals of the highest commercially available quality were used as received. NovoRapid, a zinc-free analogue of recombinant human insulin in which the Pro residue at position 28 of the β-chain is replaced with Asp, was generously provided by NovoNordisk (Bagsværd, Denmark). Zinc-free insulin was used in experiments that included Sec to avoid interference due to binding of selenium to zinc. In experiments with GSH or Cys, insulin from bovine pancreas, purchased from Sigma (Buchs SG, Switzerland) and solubilized with edta obtained from Siegfried Handel AG (Zofingen, Switzerland), was used. Selenocystine (Sec_{ox}), ammonia, and sulfuric acid were purchased from Fluka (Buchs SG, Switzerland). Sodium tetrahydroborate was purchased from Fisher Scientific (Wohlen, Switzerland). GSH was purchased from ABCR (Karlsruhe, Germany). Argon (≥99.999%) and dinitrogen monoxide (≥99.999%) were supplied by PanGas (Zürich, Switzerland). Sec (*14*) and GSeH (*20*) were prepared as previously described.

Pulse Radiolysis. A 2.3 MeV Febetron 705 accelerator from Titan Systems Corp. (San Leandro, CA) with a pulse width (full width at half-maximum) of <50 ns was used as the radiation source. Doses of 5−50 Gy/pulse were applied to a 1 cm optical path quartz cell from Hellma GmbH (Müllheim, Germany). Signals were detected with an optical system consisting of a Hamamatsu (Schüpfen, Switzerland) 75 W Xe arc lamp, an Acton SP300i monochromator from Roper Scientific (Ottobrunn, Germany), and a Hamamatsu R928 photomultiplier with a DHPCA-200 amplifier from Femto Messtechnik GmbH (Berlin, Germany), collected with a DL7100 digital storage oscilloscope from Yokogawa Electric Corp. (Tokyo, Japan). Selenol solutions were stored under acidic conditions to prevent oxidation and were mixed prior to irradiation with basic Tyr solutions to give solutions with a final pH of 11−12.

The *G* value, i.e., the number of Tyr$^•$ formed per 100 eV absorbed in a N_2O-saturated solution of >1 mM *N*-Ac-Tyr-NH_2, 100 mM NaN_3, and 1 mM KOH, is 6.1. At high pH, the initial absorbance at 400 nm represents formation of Tyr$^•$ only [ε_{400}(Tyr$^•$) = 1630 (*21*) or 1750 (*22*)], provided the concentration of *N*-Ac-Tyr-NH_2 is 100 times higher than that of Sec. At 450 nm, where $\varepsilon_{450}(Tyr^•)/\varepsilon_{400}(Tyr^•) \approx 0.1$, the initial absorbance is low and the formation of (Sec∴Sec)$^{•-}$ can be monitored [ε_{450}(Sec∴Sec)$^{•-}$ = 7.0 × 10^3 (*14*)].

Laser Flash Photolysis. Laser flash photolysis experiments were carried out with an Applied Photophysics (Leatherhead, U.K.) LKS 50 instrument equipped with a Quantel (Les Ulis, France) Brilliant B YAG laser, of which we used the fourth (5 ns, 266 nm pulses) and the third harmonics (5 ns, 355 nm pulses). A vacuum-tight fluorescence cell was used as described previously (*14*), and signals were recorded with a LeCroy (Geneva, Switzerland) WaveRunner 64Xi digital storage oscilloscope. Sec$^•$ concentrations were measured immediately after irradiation by means of UV−vis spectrometry, reported as a function of absorbance at 248 nm. The pulse energy was generally kept below 20 mJ/pulse to minimize water photolysis (*23*). Irradiation with 5 ns laser pulses at 266 nm leads to photoionization of aromatic amino acids in proteins, which allows their reactions to be followed directly (*24*). All flash photolysis experiments were carried out under N_2O to scavenge photoelectrons and in the presence of 0.1 M *tert*-butanol to scavenge any HO$^•$ generated; the concentration of *N*-Ac-Tyr-NH_2 was typically 1.5 mM, and the concentration of Cys was 10−33 mM.

Elemental Analysis. The analysis of GSH for selenium content was carried out with a PerkinElmer SCIEX (Norwalk, CT) Elan 6100 DRC ICP-MS instrument. The selenium concentration was determined by means of standard addition to control for matrix effects: the sample was dissolved in concentrated nitric acid and then diluted 1:33 in 1% (v/v) HNO_3, and the selenium signal intensity was measured at *m*/*z* 80. Interference by $^{40}Ar_2^+$ ions was reduced by addition of CH_4 to the dynamic reaction cell of the mass spectrometer according to the procedure described in detail by Hattendorf and Günther (*25*).

RESULTS

Figure 1 shows the decay of Tyr$^•$ (monitored at 400 nm) produced by pulse radiolysis of 10 mM *N*-Ac-Tyr-NH_2 with 100 mM N_3^- as a function of time in aqueous solution saturated with N_2O at pH 11−12; Tyr$^•$ radicals were generated via the reaction of trinitrogen$^•$ radicals ($N_3^•$) with the phenol and phenolate forms of *N*-Ac-Tyr-NH_2 (*26*). Tyr$^•$ radicals recombine with a rate constant of $2k = (4.5 - 12) \times 10^8$ M^{-1} s^{-1} (*21, 27*). With a dose of 9.5 Gy and a *G*

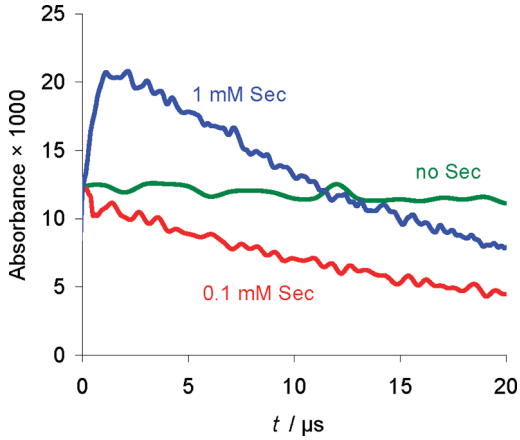

FIGURE 1: Repair of Tyr radicals by Sec. Radicals were generated by pulse radiolysis of 10 mM *N*-Ac-Tyr-NH_2 with 100 mM N_3^- in an aqueous solution saturated with N_2O at pH 11−12 at a dose of ca. 9 Gy with detection at 400 nm. The time course for the absorbance at 400 nm is shown in the absence of Sec (green) and in the presence of 0.1 mM Sec (red) and 1 mM Sec (blue). In the presence of 1 mM Sec, the species $(Sec\therefore Sec)^{\bullet-}$, which also absorbs at 400 nm, is formed.

value of 6.1, the concentration of $Tyr^\bullet$ radicals is 6 μM; given a calculated half-life for recombination of 140 μs, which is based on a worst-case scenario with $2k = 1.2 \times 10^9$ M^{-1} s^{-1}, the concentration of $Tyr^\bullet$ radicals remains nearly constant over the duration of the time scale of the experiment, 20 μs (Figure 1, green trace). In the presence of up to 0.10 mM Sec (Figure 1, red trace), the decay of the $Tyr^\bullet$ is accelerated, while the inclusion of 1 mM Sec (Figure 1, blue trace) produces an initial increase in absorbance followed by a more rapid decrease. The initial absorbance at 400 nm at pH 11−12 corresponds to quantitative production of $Tyr^\bullet$. The signal observed at 450 nm is only 10% of that at 400 nm, in agreement with the ratio $\varepsilon_{450}(Tyr^\bullet)/\varepsilon_{400}(Tyr^\bullet) \approx 0.1$.

The initial increase in absorbance observed in the presence of higher concentrations of Sec is due to equilibrium formation of $(Sec\therefore Sec)^{\bullet-}$ in reaction 2.

$$Sec^\bullet + Sec^- = (Sec\therefore Sec)^{\bullet-} \quad (2)$$

Analysis of the reactions of $(Sec\therefore Sec)^{\bullet-}$ and $Tyr^\bullet$ radicals is complicated, since these radicals have overlapping absorption spectra (*14*). Figure 2 shows the kinetics of formation and decay of $(Sec\therefore Sec)^{\bullet-}$ by pulse radiolysis at 450 nm, a wavelength at which the relative absorptivities of $(Sec\therefore Sec)^{\bullet-}$ and $Tyr^\bullet$ are optimal for detection of the former. Also here, the initial absorbance is consistent with $\varepsilon_{450}(Tyr^\bullet)/\varepsilon_{400}(Tyr^\bullet) \approx 0.1$, an indication that the majority of $N_3^\bullet$ radicals oxidized selectively Tyr over Sec (data not shown). The reaction of $Sec^\bullet$ with Sec^- was also studied by laser flash photolysis: a 1 mM solution of Sec_{ox} was subjected to photolysis at 355 nm to form Sec radicals, and the formation of $(Sec\therefore Sec)^{\bullet-}$ was followed at 450 nm in the presence of varying Sec^- concentrations. A second-order rate constant k_2 of $(2 \pm 1) \times 10^9$ M^{-1} s^{-1} for formation of $(Sec\therefore Sec)^{\bullet-}$ was derived (data not shown). To determine the equilibrium constant K_2, we measured k_{-2} by reduction of Sec_{ox} with e^-_{aq} generated by pulse radiolysis (reaction 3).

$$Sec_{ox} + e^-_{aq} \rightarrow (Sec\therefore Sec)^{\bullet-} \quad (3)$$

Relaxation to equilibrium 2 follows the rate law $k_{obs} = k_2[Sec^-] + k_{-2}$. In the absence of added Sec^- and at low doses, $k_2[Sec^-] \ll k_{-2}$, and therefore, $k_{obs} = k_{-2}$; the observed decay directly represents $k_{-2} = (1.1 \pm 0.1) \times 10^6$ s^{-1} (data not shown).

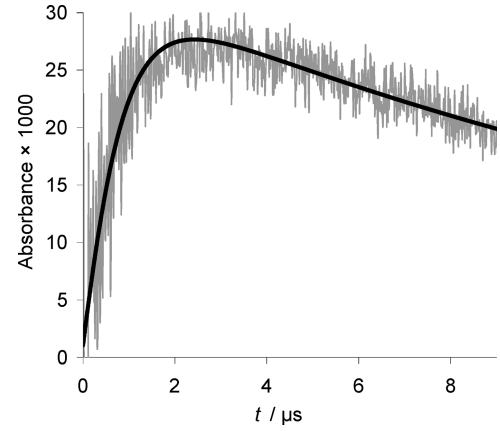

FIGURE 2: Formation and decay of $(Sec\therefore Sec)^{\bullet-}$. Radicals were generated by pulse radiolysis of 10 mM *N*-Ac-Tyr-NH_2 in the presence of 1 mM Sec with 100 mM N_3^- in an aqueous solution saturated with N_2O at pH 11−12 and a dose of 10.6 Gy with detection at 450 nm. The main absorbing species at 450 nm is $(Sec\therefore Sec)^{\bullet-}$, predominantly formed via reaction 1 and equilibrium 2. The solid line is a fit generated with a k_1 of 1×10^9 M^{-1} s^{-1}, a k_2 of 2×10^9 M^{-1} s^{-1}, a k_4/k_5 of 2, a first-order rate constant k of 8×10^4 s^{-1} (see text) for the absorbance decay, and absorptivities reported in the literature (*14, 21*).

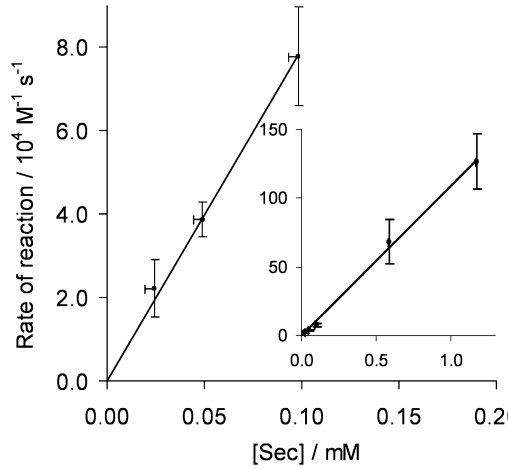

FIGURE 3: Pseudo-first-order rate constant (k_{obs}) for repair of Tyr radicals as a function of Sec concentration. Radicals were generated by pulse radiolysis as described in Figures 1 and 2, with detection at 400 nm. A second-order rate constant of $(8 \pm 2) \times 10^8$ M^{-1} s^{-1} is calculated for concentrations of up to 0.1 mM Sec; the relative uncertainty in the Sec concentration at lower initial concentrations of Sec, which is higher due to oxidation by dioxygen, is indicated with horizontal error bars. The identical rate constant was determined at higher concentrations of Sec (see inset), after correction of the absorbance at 400 nm for the formation and decay of $(Sec\therefore Sec)^{\bullet-}$.

Analysis of the dependence of the rate of reaction 1 on the concentration of Sec up to 0.1 mM (Figure 3) allowed the second-order rate constant of $(8 \pm 2) \times 10^8$ M^{-1} s^{-1} to be derived. At higher concentrations of Sec, the oxidation of Sec by $N_3^\bullet$, which we assume to be at least as fast as that of Cys,[2] must be taken into account, together with the formation and subsequent decay of $(Sec\therefore Sec)^{\bullet-}$. This decay

[2] Preliminary results indicate that the rate constant of the oxidation of Sec by $N_3^\bullet$ is $(4 \pm 1) \times 10^9$ M^{-1} s^{-1}.

Table 1: Rate Constants for Repair of Tyrosyl Radicals (as *N*-Ac-Tyr-NH_2 and in insulin) with GSH, Cys, GSeH, and Sec at pH 7.4

	N-Ac-Tyr-NH_2		insulin	
repair molecule	concentration (mM)	k (M^{-1} s^{-1})	concentration (mM)	k (M^{-1} s^{-1})
Sec	0.01–0.1	$(8 \pm 2) \times 10^{8a}$	0.05–0.3	$(1.6 \pm 0.8) \times 10^{8a}$
GSeH	0.01–0.06	$(5 \pm 2) \times 10^{8a}$	0.04–0.1	$(4.0 \pm 3) \times 10^{6a}$
Cys	10–33	$(6 \pm 3) \times 10^{5}$	1–3	$(1.0 \pm 0.6) \times 10^{5}$
GSH	10–200	$(2.4 \pm 1.6) \times 10^{3b}$	4–13	$(1.0 \pm 0.6) \times 10^{4}$

[a] Observed rate constant at pH 7.4−12. [b] From ref *28*. At pH 7.0−7.4.

was approximated with a first-order function for the first 20% of the absorbance change as a purely mathematical construct (Figure 2). The resulting rate constant for the tyrosyl radical reduction by selenocysteine ($k_1 = 1 \times 10^9$ M^{-1} s^{-1}) is in agreement with the value obtained more directly at lower concentrations of Sec (Figure 3, inset).

Since amino acids that contain sulfur and selenium have comparable biological functions, we compared the reactivities of *N*-Ac-Tyr$^{\bullet}$-NH_2 with Cys, Sec, GSH, and GSeH. Sec and GSeH are strikingly more reactive than their sulfur analogues (Table 1). The rate constants for the reaction of Sec and GSeH with Tyr$^{\bullet}$ were obtained by means of pulse radiolysis as outlined above. Although pulse radiolysis has the advantage of permitting quantitative assessment of yields, the method is inconvenient under conditions of higher concentrations of Cys and GSH, which are less reactive, since too many oxidizing equivalents are directly diverted to sulfur. The flash photolysis technique, which allows tyrosine to be photoionized selectively, was used to determine rate constants of repair by sulfur compounds. Rate constants for the reaction of Tyr (1.5 mM) with Cys (10−33 mM) were determined by analyzing the decay of the Tyr$^{\bullet}$ radical at 330 nm by laser flash photolysis; a previously determined rate constant for reaction of the Tyr$^{\bullet}$ radical with GSH (*28*), also obtained by laser flash photolysis, is included for comparison.

To determine whether Sec can repair Tyr$^{\bullet}$ in proteins, we performed analogous experiments with insulin by flash photolysis. Insulin (10 μM) was photoionized in the presence and absence of 3 mM GSH, 1 mM Cys, 1 mM GSeH, or 0.1 mM Sec at pH 7.4, and the decay of Tyr$^{\bullet}$ radicals was followed at 410 nm (see Figure 4). The rate constant determined for the reaction of insulin Tyr$^{\bullet}$ radicals with Sec is $(1.6 \pm 0.4) \times 10^8$ M^{-1} s^{-1}, similar to that for the reaction of Sec with free *N*-Ac-Tyr-NH_2 radicals. In comparison, Cys, at a concentration 10-fold higher than that of Sec, reacts considerably more slowly, with a rate constant k of $(1.0 \pm 0.3) \times 10^5$ M^{-1} s^{-1}. Similarly, while moderate repair of Tyr$^{\bullet}$ radicals in the presence of 1 mM GSeH is observed, no repair at all can be observed over the time scale of the experiment in presence of 3 mM GSH; the difference in reactivity is similar, with rate constants (k) of $(4 \pm 2) \times 10^6$ M^{-1} s^{-1} for GSeH and $(1.0 \pm 0.3) \times 10^4$ M^{-1} s^{-1} for GSH.

The selenium content of GSH was determined to examine the possibility of interference by trace levels of selenium: a level of 7 ± 1 ng/g (95%) corresponds to a molar Se/S ratio of ca. 10^{-7}, which is insufficient to account for the difference in reactivity.

DISCUSSION

The findings presented herein show that Sec reacts rapidly with tyrosyl radicals in both *N*-Ac-Tyr-NH_2 and protein (insulin) with second-order rate constants on the order of

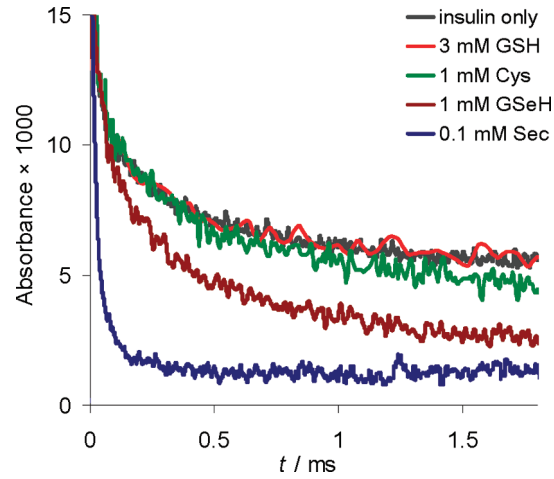

FIGURE 4: Repair of tyrosyl radicals in insulin by Cys, Sec, GSH, and GSeH. Laser flash photolysis of 10^{-5} M zinc-free insulin in the absence and presence of selenium and sulfur compounds at the indicated concentrations in aqueous solution saturated with N_2O at pH 7.40, with 1 mM edta and 0.1 M *tert*-BuOH present. The tyrosyl radical concentration was followed at 410 nm. Tyrosyl radical repair in insulin by Sec is rapid with a rate constant k of $(1.6 \pm 0.8) \times 10^8$ M^{-1} s^{-1}, while repair by Cys is 3 orders of magnitude slower. Repair by GSH is 4 orders of magnitude slower than that by GSeH; with 3 mM GSH over the time scale of the figure, no repair can be detected.

10^8−10^9 M^{-1} s^{-1}. This high rate constant, compared to the rate constant for the reaction of *N*-Ac-Tyr-NH_2 with Cys that is more than 3 orders of magnitude smaller, strikingly reflects the accessibility of the selenium radical oxidation state (*14*).

The reaction pathway and the absorbance−time profiles are dependent on the Sec/Tyr concentration ratio. The production of the initial oxidant, $N_3^{\bullet}$, is linearly dependent on the dose and is characterized by a G value of 6.1. With 10 mM Tyr at pH 12, the half-life for formation of the Tyr$^{\bullet}$ radical is 20 ns (*26*), which, for our purposes, can be considered instantaneous, but not *a priori* quantitative. If Tyr$^{\bullet}$ radicals are produced quantitatively, the initial absorbance at 400 nm in the time profiles must be identical for all experiments performed at a given dose, and this was the case for experiments carried out at pH >11 and <1 mM Sec. Quantitative formation of Tyr$^{\bullet}$ is also indicated by the observation that the ratio of the initial absorbance of Tyr$^{\bullet}$ at 450 nm to that at 400 nm is ≈0.1, corresponding to an ε_{450}(Tyr$^{\bullet}$)/ε_{400}(Tyr$^{\bullet}$) of ≈0.1. As expected, the rate constants derived at these wavelengths are the same. However, at pH 7.4, $N_3^{\bullet}$ oxidizes Sec^- with a rate constant higher than that of Tyr ($k_5 > k_4$), and the reaction of $N_3^{\bullet}$ with Sec^- prevails at much lower Sec concentrations.

$$N_3^{\bullet} + Tyr^- \rightarrow N_3^- + Tyr^{\bullet} \quad (4)$$

$$N_3^{\bullet} + Sec^- \rightarrow N_3^- + Sec^{\bullet} \quad (5)$$

To derive a reliable rate constant for repair of Tyr$^{\bullet}$ by Sec, it is essential to obtain rate data over a wide range of Sec concentrations, but, because of reaction 5, which competes with reaction 4, quantitative production of Tyr$^{\bullet}$ radicals cannot be ensured over such a wide concentration range at neutral pH. Sec is deprotonated at neutral pH, and the rate constant for transfer of an electron from Sec to Tyr$^{\bullet}$ should be independent of pH from pH 7.4 to ~12, provided that reaction 1 is elementary and rate-determining. Indeed, we found experimentally that, within this pH range, the reaction rate is independent of pH. Thus, the change in electrode potential of the TyrO$^{\bullet}$/TyrOH couple of ca. 0.2 V (*29*) does not influence the rate of electron transfer. At pH >10, Tyr is deprotonated and k_4 is sufficiently high to allow collection of meaningful rate data over a 1 order of magnitude range of Sec concentrations. We, therefore, carried out the majority of experiments at pH 11−12.

The shape of the absorbance profile at 400 nm as a function of time, i.e., that for formation of Tyr$^{\bullet}$, is strongly influenced by equilibrium 2, because the absorptivity of $(Sec)_2^{\bullet-}$ at this wavelength is much larger than that of Tyr$^{\bullet}$. As a consequence, when the concentration of Sec is increased to millimolar levels, the production of $(Sec)_2^{\bullet-}$ increasingly influences the absorbance versus time profiles. Thus, below 0.1 mM Sec, the reduction of Tyr$^{\bullet}$ radicals produces a decay in absorbance because Tyr$^{\bullet}$ radicals are the predominant absorbing species. At concentrations of Sec of ≥1 mM, equilibrium 2 lies to the right and the main absorbing species is $(Sec\therefore Sec)^{\bullet-}$. Because the absorptivity of $(Sec)_2^{\bullet-}$ is greater than that of the Tyr$^{\bullet}$ radical, an increase in absorbance is observed. Formation of $(Sec\therefore Sec)^{\bullet-}$ lags behind that of Sec$^{\bullet}$, and $(Sec\therefore Sec)^{\bullet-}$ decays so rapidly that the kinetics of formation cannot be treated as a process completely separated from decay. The determination of k_1 is, thus, dependent on several parameters, and the treatment of data collected at high Sec concentrations entails more uncertainty; however, the results may be viewed as verification of those obtained at lower Sec concentrations. Although $(Sec\therefore Sec)^{\bullet-}$ is more reducing than Sec (*14*), the concentration of $(Sec\therefore Sec)^{\bullet-}$ in these experiments never exceeds the micromolar range, and the reaction with tyrosyl radicals is negligible. The experimentally determined equilibrium constant [$K_2 = (2 \pm 1) \times 10^3$ M^{-1}] is 1 order of magnitude lower than our earlier estimate of 1.7×10^4 M^{-1} (*14*).

The rate constant for the reaction of GSeH with *N*-Ac-Tyr-NH_2 is 5 orders of magnitude higher than that of GSH, and we reasoned that minor contamination of GSH with GSeH could be responsible for part or all of the reactivity in the GSH sample. The Se content of the GSH used in our rate determinations is 7 ± 1 ng/g at the 95% confidence level and corresponds to a molar Se/S ratio of ca. 10^{-7}, which is too low for the reactivity of GSH reported here to be entirely due to contaminating Se. However, nonspecific biological replacement of sulfur with selenium (*30*) could enhance the apparent reactivities of Cys and GSH in vivo.

During the 1980s, it was established (*4, 6, 31*) that one-electron oxidation of residues in proteins results in chain reactions in which ultimately Tyr$^{\bullet}$ radicals are formed. We show here that repair of Tyr$^{\bullet}$ residues in insulin by Sec is nearly as rapid as that of Tyr$^{\bullet}$, as *N*-Ac-Tyr-NH_2, in solution. Protein radical repair by Sec results in the formation of Sec$^{\bullet}$, which may be converted to Sec_{ox} or a selenodisulfide, and superoxide; the latter can be eliminated via the superoxide-sink pathway (*15*). It should be noted that the concentration of Sec in aqueous compartments of the cell is very low, much lower than that of ascorbate, and that the latter is much more likely to effect repair of protein radicals. However, in the microscopic environment of a selenoprotein, the effective concentration of Sec residues is higher, and a protective function, namely repair of radical damage to neighboring residues, can be postulated. Cys and Sec are usually found in hydrophobic parts of proteins. Furthermore, many selenoproteins have redox functions, and we do not exclude the possibility that, in cellular compartments with high concentrations of selenoproteins, these proteins act as radical scavengers. Intriguingly, in recent studies, selenoproteins have been shown to protect against oxidative stress (*32*). We have shown that Sec is a very potent radical scavenger, a property that may contribute to the beneficial effects of dietary selenium against cancer, cardiovascular diseases, and neurodegenerative diseases, as well the aging process.

ACKNOWLEDGMENT

We thank Prof. D. Hilvert for his support of this investigation, and we gratefully acknowledge Nova Nordisk for supplying zinc-free insulin.

REFERENCES

1. Connelly, N. G., Damhus, T., Hartshorn, R. M., and Hutton, A. T. (2005) *Nomenclature of Inorganic Chemistry. IUPAC Recommendations 2005*, Royal Society of Chemistry, Cambridge, U.K.
2. Buettner, G. R. (1993) The pecking order of free radicals and antioxidants. Lipid peroxidation, α-tocopherol, and ascorbate. *Arch. Biochem. Biophys. 300*, 535–543.
3. Prütz, W. A., Butler, J., Land, E. J., and Swallow, A. J. (1980) Direct demonstration of electron transfer between tryptophan and tyrosine in proteins. *Biochem. Biophys. Res. Commun. 96*, 408–414.
4. Prütz, W. A., Siebert, F., Butler, J., Land, E. J., Menez, A., and Montenay-Garestier, T. (1982) Intramolecular radical transformations involving methionine, tryptophan and tyrosine. *Biochim. Biophys. Acta 705*, 139–149.
5. Prütz, W. A., Butler, J., and Land, E. J. (1985) Methionyl → tyrosyl radical transitions initiated by $Br_2^{\bullet-}$ in peptide model systems and ribonuclease A. *Int. J. Radiat. Biol. 47*, 149–156.
6. Prütz, W. A., Butler, J., Land, E. J., and Swallow, A. J. (1986) Unpaired electron migration between aromatic and sulfur peptide units. *Free Radical Res. Commun. 2*, 69–75.
7. Heinecke, J. W. (2002) Tyrosyl radical production by myeloperoxidase: A phagocyte pathway for lipid peroxidation and dityrosine cross-linking of proteins. *Toxicology 177*, 11–22.
8. Hunter, P. L., Desrosiers, M. F., and Simic, M. G. (1989) The effect of oxygen, antioxidants, and superoxide radical on tyrosine phenoxyl radical dimerization. *Free Radical Biol. Med. 6*, 581–585.
9. Stubbe, J., and van der Donk, W. A. (1998) Protein radicals in enzyme catalysis. *Chem. Rev. 98*, 705–762.
10. Ito, N., Phillips, S. E. V., Stevens, C., Ogel, Z. B., McPherson, M. J., Keen, J. N., Yadav, K. D. S., and Knowles, P. (1991) Novel thioether bond revealed by a 1.7 Å crystal structure of galactose oxidase. *Nature 350*, 87–90.
11. Bravo, J., Fita, I., Ferrer, J. C., Ens, W., Hillar, A., Switala, J., and Loewen, P. C. (1997) Identification of a novel bond between a histidine and the essential tyrosine in catalase HPII of Escherichia coli. *Protein Sci. 6*, 1016–1023.
12. Buse, G., Soulimane, T., Dewor, M., Meyer, H. E., and Blüggel, M. (1999) Evidence for a copper-coordinated histidine-tyrosine cross-link in the active site of cytochrome oxidase. *Protein Sci. 8*, 985–990.
13. Rauhamäki, V., Baumann, M., Soliyman, R., Puustinen, A., and Wikström, M. (2006) Identification of a histidine-tyrosine crosslink in the active site of the *cbb*$_3$-type cytochrome *c* oxidase from

Rhodobacter sphaeroides. *Proc. Natl. Acad. Sci. U.S.A. 103*, 16135–16140.
14. Nauser, T., Dockheer, S., Kissner, R., and Koppenol, W. H. (2006) Catalysis of electron transfer by selenocysteine. *Biochemistry 45*, 6038–6043.
15. Winterbourn, C. C. (1993) Superoxide as an intracellular radical sink. *Free Radical Biol. Med. 14*, 85–90.
16. Koppenol, W. H. (1993) A thermodynamic appraisal of the radical sink theory. *Free Radical Biol. Med. 14*, 91–94.
17. Copeland, P. R. (2005) Making sense of nonsense: The evolution of selenocysteine usage in proteins. *Genome Biol. 6*, 221.
18. Kryukov, G. V., Castellano, S., Novoselov, S. V., Lobanov, A. V., Zehtab, O., Guigó, R., and Gladyshev, V. N. (2003) Characterization of mammalian selenoproteomes. *Science 300*, 1439–1443.
19. Gromer, S., Eubel, J. K., Lee, B. L., and Jacob, J. (2005) Human selenoproteins at a glance. *Cell. Mol. Life Sci. 62*, 2414–2437.
20. Beld, J., Woycechowsky, K. J., and Hilvert, D. (2007) Selenoglutathione: Efficient oxidative protein folding by a diselenide. *Biochemistry 46*, 5382–5390.
21. Feitelson, J., and Hayon, E. (1973) Electron ejection and electron capture by phenolic compounds. *J. Phys. Chem. 77*, 10–15.
22. Bansal, K. M., and Fessenden, R. W. (1976) Pulse radiolysis studies of the oxidation of phenols by SO_4^- and Br_2^- in aqueous solutions. *Radiat. Res. 67*, 1–8.
23. Reuther, A., Lauberau, A., and Nikogosyan, D. N. (1996) Primary photochemical processes in water. *J. Phys. Chem. 100*, 16794–16800.
24. Grossweiner, L. I., Kaluskar, A. G., and Baugher, J. F. (1976) Flash photolysis of enzymes. *Int. J. Radiat. Biol. 29*, 1–16.
25. Hattendorf, B., and Günther, D. (2003) Strategies for method development for an inductively coupled plasma mass spectrometer with bandpass reaction cell. Approaches with different reaction gases for the determination of selenium. *Spectrochim. Acta, Part B 58*, 1–13.
26. Land, E. J., and Prütz, W. A. (1979) Reaction of azide radicals with amino acids and proteins. *Int. J. Radiat. Biol. 36*, 75–83.
27. Jin, F., Leitich, J., and von Sonntag, C. (1993) The superoxide radical reacts with tyrosine derived phenoxyl radicals by addition, rather than by electron transfer. *J. Chem. Soc., Perkin Trans. 2*, 1583–1588.
28. Nauser, T., Koppenol, W. H., and Gebicki, J. M. (2005) The mechanism and kinetics of the oxidation of GSH by protein free radicals. *Biochem. J. 392*, 693–701.
29. Prütz, W. A., Butler, J., Land, E. J., and Swallow, A. J. (1989) The role of sulphur peptide functions in free radical transfer: A pulse radiolysis study. *Int. J. Radiat. Biol. 55*, 539–556.
30. Müller, S., Heider, J., and Böck, A. (1997) The path of unspecific incorporation of selenium in *Escherichia coli*. *Arch. Microbiol. 168*, 421–427.
31. Butler, J., Land, E. J., Prütz, W. A., and Swallow, A. J. (1986) Reversibility of charge transfer between tryptophan and tyrosine. *J. Chem. Soc., Chem. Commun.,* 348–349.
32. Brenneisen, P., Steinbrenner, H., and Sies, H. (2005) Selenium, oxidative stress, and health aspects. *Mol. Aspects Med. 26*, 256–267.

BI801029F